

Ferromagnetic elements by epitaxial growth: A density functional prediction

Stephan Schönecker,* Manuel Richter, Klaus Koepf, and Helmut Eschrig

IFW Dresden, P.O. Box 270116, D-01171 Dresden, Germany

(Received 27 December 2011; published 10 January 2012; publisher error corrected 3 December 2012)

The periodic table contains only six natural elements with a ferromagnetic ground state. For example, the metal uranium, which is magnetically ordered in many compounds, is paramagnetic in all its known elemental bulk phases. Also, the iron-group elements ruthenium and osmium are known to be bulk paramagnets. We predict by means of density functional calculations that epitaxial growth of uranium, ruthenium, or osmium on suitable substrates may allow stabilization of bulklike films with tetragonal structures showing ferromagnetic order.

DOI: [10.1103/PhysRevB.85.024407](https://doi.org/10.1103/PhysRevB.85.024407)

PACS number(s): 71.20.-b, 75.50.Cc

I. INTRODUCTION

Ferromagnetism is an important but rare state of matter. Only six natural elements are known to be ferromagnetic in their bulk ground state, while 29 natural elements¹ with a superconducting bulk ground state at ambient pressure have been identified, hitherto. The six ferromagnetic elements are 3*d* transition metals (Fe, Co, Ni) or belong to the 4*f* lanthanide series (Gd, Dy, Tb). There is no natural element among the 5*f* actinides or the 4*d* or 5*d* transition metals known to be ferromagnetic in the bulk.

Magnetism among uranium *compounds* is not unusual, though. Indeed, such compounds exhibit different types of magnetic order ranging from ferromagnetic order in US over antiferromagnetic order in UN (Ref. 2) to canted order in U₃P₄.³ Yet more intriguing, coexistence of ferromagnetism and superconductivity was found in UCoGe.⁴ These phenomena reflect the active role of U 5*f* electrons in forming a broken-symmetry ground state.

Bulk elemental uranium in its orthorhombic ground-state structure, on the other hand, is a paramagnet. This α phase is stable up to temperatures of 940 K.⁵ At temperatures below 43 K, α -U undergoes three structural phase transitions manifesting themselves in charge-density waves (CDWs).⁶ Apart from a complex tetragonal high-temperature phase, experiments revealed a body-centered-cubic (bcc) phase, stable above 1045 K.⁷

The picture that has evolved for uranium by comparison of experimental data with density functional theory (DFT) describes the 5*f* electrons as weakly to moderately correlated itinerant electrons contributing to chemical bonding.^{6,8,9} For example, DFT confirms the 43 K CDW state.¹⁰ Quasiparticle GW calculations for α -U showed that self-energy corrections mainly affect the excited-state spectra, not the occupied band structure below the Fermi energy or ground-state properties.¹¹ In this context, recent DFT calculations indicated that in thin α -U-like films thicker than one monolayer the *surface* layer is probably magnetic.^{12,13} The occurrence of surface magnetism was traced back to a fulfilled Stoner criterion caused by the narrower bands and the increased density of states (DOS) at the surface compared to the bulk counterpart.

Recent experimental progress has been achieved in the epitaxial growth of uranium films, including the manufacture of hexagonal close-packed (hcp) metastable bulklike¹⁴ films up to 50 nm thickness.^{15–17} Notably, an hcp structure is not known from the conventional pressure-temperature phase diagram

of uranium.⁷ Ferromagnetic order was found for bulk hcp U by DFT calculations,¹⁷ but this prediction has not been confirmed hitherto. It is therefore tempting to focus attention on heteroepitaxial growth of films with alternative, e.g., body-centered tetragonal (bct), structures. Such an attempt includes bcc U films aimed at in earlier growth experiments.¹⁷

Ruthenium and osmium, both in the iron group, crystallize in hcp structures and are paramagnetic, like uranium, in their bulk phases. Blügel predicted, by means of DFT calculations, ferromagnetic states for *monolayers* of Ru on Ag(001) and Au(001) and of Os on Ag(001).¹⁸ Later, Watanabe *et al.* carried out DFT calculations for bulk bct Ru with fixed lattice parameter ratios c/a but variable volume and obtained ferromagnetic solutions at $c/a < 1$.¹⁹ Formation of 5–10 nm bct Ru films on Mo(110) had been reported before, but their magnetic properties were not considered.²⁰ We are not aware of related results for bulklike films of Os.

An appropriate theoretical frame for the study of epitaxial bct overlayers is the epitaxial Bain path (EBP).^{21,22} The EBP model assumes that a thick, bulklike film grows coherently on a substrate with fourfold symmetry. Thus, the in-plane film lattice parameter a is biaxially strained to fit the substrate dimensions, resulting in tetragonal overlayers encountering isotropic stress in the (001) plane and vanishing out-of-plane stress along [001]. The out-of-plane lattice constant c is obtained by minimizing the total energy $E(a', c')$ with respect to c' , and $E(a) \stackrel{\text{def}}{=} E(a, c(a)) = \min_{c'} E(a', c')|_{a'=a}$. The function $E(a)$ is stationary at the points with $c/a = 1$ (bcc) and $c/a = \sqrt{2}$ (face-centered cubic, fcc);²² see Fig. 1 for an example.

If the strain energy, $E(a) - E_0$ with E_0 denoting the energy of the stable phase, is small enough compared to the energy barrier for introducing misfit dislocations, highly strained films can be stabilized in a variety of crystal structures.^{23–25} For example, experimentalists succeeded in stabilizing bct Co films on various substrates with axial ratios c/a from 0.94 to 1.45, covering not only the EBP range between bcc and fcc, but also beyond; see Ref. 26 and references therein. It is notable that this range includes a bct state at a local minimum of $E(a)$, which was shown to be unstable in the bulk according to conventional elasticity theory.²²

In the present work, we check by DFT the possibility of ferromagnetic ground states in bulklike films of uranium and of *all* transition metal elements which are not ferromagnetic in their bulk structures. We indeed find large regions of

ferromagnetic solutions along the EBP for three elements, U, Ru, and Os. The feasibility of preparing sufficiently thick films is investigated by calculating the related strain energy.

II. NUMERICAL DETAILS

The DFT calculations were carried out with the full-potential local-orbital scheme FPLO-9.00-34.²⁷ The generalized gradient approximation (GGA) in the parametrization according to Ref. 28 was used and the results were cross-checked with the local spin density approximation; see below.

Convergence of the numerical parameters and basis was carefully checked. Linear-tetrahedron integrations with Blöchl corrections on a $24 \times 24 \times 24$ mesh in the full Brillouin zone, used for reported structural properties, were sufficient to converge the total energy at a level of $50 \mu\text{eV}$ compared to a $48 \times 48 \times 48$ mesh. The reported DOSs and magnetic moments were obtained with the latter mesh. The valence basis comprised $5df$, $6spdf$, $7spd$, and $8s$ states in the case of U; $4spd$, $5spd$, and $6s$ states for Ru; $5spd$, $6spd$, and $7s$ states for Os.

The bct films were modeled by the space group $I4/mmm$. The scalar-relativistic mode was employed for ruthenium, the fully relativistic mode for osmium and uranium. To account for the possibility of ferromagnetic order in the evaluation of the EBP, total energy minimization was done with respect to both c and the magnetic moment. A few antiferromagnetic states were checked and found to be higher in energy than the ferromagnetic ground states; see below. The tetragonal axis was chosen as quantization axis. All reported volumes, energies, and moments are given per atom.

Reference calculations were performed for the orthorhombic α -uranium structure (space group $Cmcm$) and the hcp structure (space group $P6_3/mmc$), prepared in previous experiments on epitaxial uranium films.^{15–17} For α -U we obtain $a = 2.840 \text{ \AA}$, $b = 5.829 \text{ \AA}$, $c = 4.962 \text{ \AA}$ ($V_{\alpha\text{-U}} = 20.537 \text{ \AA}^3$), and $y = 0.1008 \text{ \AA}$ in good agreement with experiment.⁵ Charge-density waves in α -uranium were neglected due to their small energy scale of less than 1 meV .¹⁰ For hcp U, the energy is lowest for $a = 3.009 \text{ \AA}$ and $c/a = 1.820$. As expected, it is higher than the total energy of α -U, $E_{\text{hcp U}} - E_{\alpha\text{-U}} = 0.19 \text{ eV}$. Both the unusually large c/a and the energy difference agree well with values from a published calculation, $c/a = 1.84$ and $E_{\text{hcp U}} - E_{\alpha\text{-U}} = 0.21 \text{ eV}$.¹⁷ In the experiment, the in-plane lattice parameter of hcp U was determined to be $a = 2.96 \text{ \AA}$,¹⁷ pointing to a small negative in-plane strain of the uranium film deposited on a gadolinium substrate. We calculated the relaxed c/a ratio for $a = 2.96 \text{ \AA}$ and found $c/a = 1.864$, close to the measured value, $c/a = 1.90(1)$. The energy difference of this strained hcp structure compared to the unstrained hcp U amounts to 16 meV . The relaxed geometries for the hcp phases of Ru and Os are $a = 2.730 \text{ \AA}$ and $c/a = 1.58$ and $a = 2.759 \text{ \AA}$ and $c/a = 1.58$, respectively.

III. RESULTS AND DISCUSSION

The total energy $E(a)$ of uranium, Fig. 1, contains three minima along the EBP. The maxima correspond to the bcc and fcc structures. Qualitatively, the same rich structure was obtained earlier by Söderlind, who reported results of

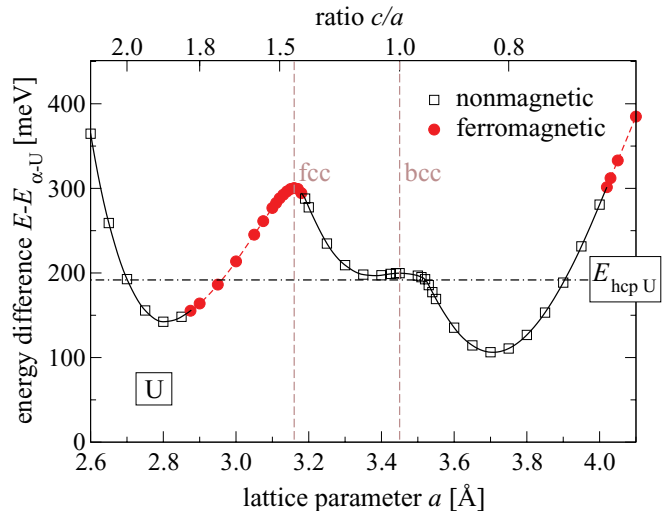


FIG. 1. (Color online) Total energy of uranium with respect to the energy of the stable phase $E_0 \equiv E_{\alpha\text{-U}}$ for states along the EBP. The lines are spline interpolations to the data and serve as guides to the eye. $E_{\text{hcp U}}$ is indicated by a horizontal line. Nonmagnetic states are omitted in regions where ferromagnetic states are lower in energy.

nonmagnetic calculations constrained to the experimental volume.³⁰ Moreover, the positions and numerical values of the extrema agree well with the literature data; see Table I. The extrapolated low-temperature lattice parameter of bcc uranium, 3.474 \AA ,⁷ is close to our calculated value, 3.45 \AA . The total energies of hcp U and of bcc U are close to each other and well above the two pronounced minima at the flanks of the EBP. From this fact and the reported experimental realization of 50-nm-thick hcp U films, we conclude that it should be possible to grow *bulklike*¹⁴ tetragonal uranium films on substrates in a wide a range between about 2.6 and 4.0 \AA .

Turning our attention to possible magnetic states we note that according to our calculations neither the α -U nor the hcp U shows a stable ferromagnetic state. The authors of Ref. 17 reported that in their full potential linear muffin tin orbital (FP-LMTO) calculations bulk hcp uranium would be ferromagnetic with a total moment of $0.12 \mu_B$. We could not reproduce this magnetic state, although the optimized structural parameters are very similar in our and their calculations. The absence of

TABLE I. Positions and values of all extrema on the EBP of uranium ordered by increasing a (decreasing c/a). The extrema are referred to as their highest symmetry indicates; bct structures are consecutively numbered. Type defines the type of extremum along the EBP (min = minimum and max = maximum in total energy). Differences in energy with respect to the ground state are compared to GGA values available in the literature.

	Type	a (\AA)	c/a	$E - E_{\alpha\text{-U}}$ (meV)
bct ⁽¹⁾	min	2.80	1.89	142
fcc	max	3.16	1.41	300, 259 ^a
bct ⁽²⁾	min	3.38	1.07	197
bcc	max	3.45, 3.46 ^a	1.00	200, 223 ^a
bct ⁽³⁾	min	3.70	0.82	106, 92.5 ^{a,b}

^aGGA values in FP-LMTO calculation; Ref. 8.

^bWith fixed $c/a = 0.825$.

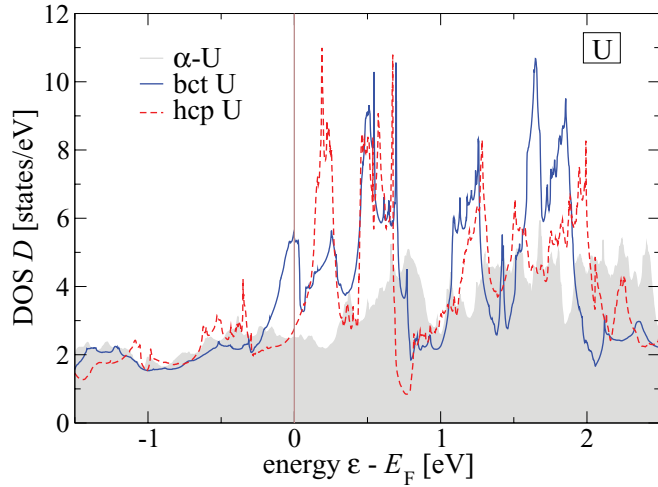


FIG. 2. (Color online) Total DOSs of α -U (shaded), hcp U (broken line), and bct U (full line) at $a = 3.00 \text{ \AA}$, nonmagnetic mode. The Fermi energy is indicated by a vertical line.

ferromagnetic magnetic order in hcp U is in accordance with the relatively small value of the hcp DOS at the Fermi level (cf. Figs. 2 and 4), which we computed to 2.75 states/eV. The DOS of hcp uranium exhibits a strong peak 0.16 eV above E_F , Fig. 2, which could become crucial for strained hcp uranium. To test this possibility, we applied a maximum in-plane strain of 0.045 on the relaxed hcp structure, both compressive and tensile, with accompanied relaxation of the c coordinate. We found that magnetism is absent for such strained hcp lattices of uranium as well.

However, ferromagnetic order is surprisingly revealed for two regions of the EBP, $2.875 \leq a \leq 3.18 \text{ \AA}$ and $a \geq 4.02 \text{ \AA}$; Fig. 1. States in the second region are high in energy and also exhibit large in-plane stresses $\sigma = 2|\partial E/\partial a|/(ac)$.²² From the experimental point of view, the feasibility of epitaxial growth depends on both parameters, $E - E_{\alpha\text{-U}}$ and σ , in the sense that the smaller the better.²⁴ Thus, realization of magnetic bct U films is realistic in the first region, but more difficult in the second one.

Figure 3 shows the energy difference between nonmagnetic and ferromagnetic states of bct U vs a . Its magnitude suggests that ferromagnetism could be stable at temperatures of several 10 K. Figure 3 also displays data of spin, orbital, and total magnetic moments for ferromagnetic bct U. Both spin and orbital moments are of considerable magnitude, but couple antiparallel and almost cancel each other. The remaining total moment amounts to $(0.2\text{--}0.3)\mu_B$. The large orbital moment originates from the strong spin-orbit coupling in the narrow $5f$ band of uranium.³⁰ It can be yet larger in reality due to orbital polarization, which is not considered here.

To answer the question of what drives the onset of magnetism in certain tetragonal states, we consider the DOS at the Fermi level, $D(E_F)$, vs a ; see Fig. 4. $D(E_F)$ shows great variability along the EBP with peak values more than twice as large as the ground-state DOS, $D_{\alpha\text{-U}}(E_F) = 2.5 \text{ states/eV}$. Similar values for $D_{\alpha\text{-U}}$ can be found in the literature.^{8,11} We note in Fig. 4 that $D_{5f}(E_F) > 3.5 \text{ states/eV}$ in the ferromagnetic regions, while it is smaller outside. The Stoner criterion for the onset of magnetism, $ID(E_F) \geq 1$, with the Stoner

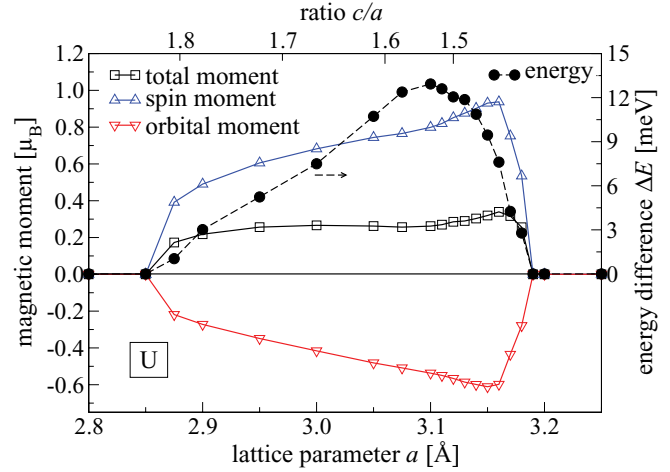


FIG. 3. (Color online) Total, spin, and orbital magnetic moments for the magnetic states of the EBP of uranium, left-hand axis, and total energy difference $\Delta E = E(\text{non-spin-polarized}) - E(\text{spin-polarized})$, right-hand axis. Lines guide the eye. Note that relaxation of c yields different values for magnetic and nonmagnetic states. Thus, c/a gives approximate values.

exchange integral $I_{U5f} \approx 0.2 \text{ eV}$,^{13,31} is *not* fulfilled in the whole ferromagnetic region but only in its central parts. In the other parts of the ferromagnetic region, a nontrivial situation³² with a metastable nonmagnetic and a stable ferromagnetic state is obviously present.

It has been argued^{29,33,34} that the narrower bandwidth of the dominant $5f$ band in uranium compared to the d bandwidth in a transition metal is the decisive factor causing uranium to crystallize in a low-symmetric, open crystal structure. The mechanism that stabilizes such open structures is considered to be similar to a Peierls or Jahn-Teller distortion. Metals

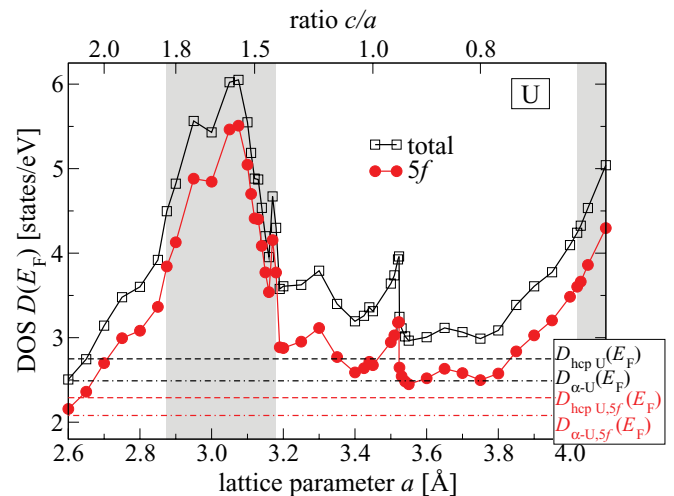


FIG. 4. (Color online) Total and $5f$ -projected DOSs at the Fermi energy E_F , $D(E_F)$, for the states along the EBP of uranium, calculated in the non-spin-polarized mode. The solid lines guide the eye. The difference between the two curves can be almost exclusively attributed to $6d$ states (not shown). The gray bar indicates the region of ferromagnetic states of the EBP, Fig. 1. Horizontal dash-dotted and dotted lines mark the corresponding total and $5f$ -projected values of hcp U and of α -U, respectively.

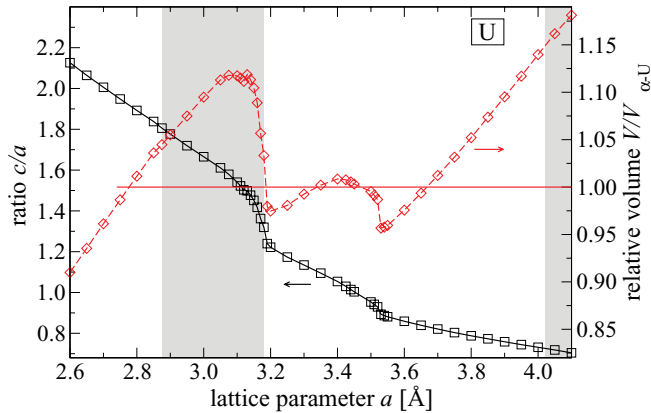


FIG. 5. (Color online) Lattice parameter ratio c/a and relative volume for the EBP of uranium. The volume is given with respect to $V_{\alpha-U}$, and the horizontal red (gray) line indicates $V/V_{\alpha-U} = 1$. The other lines guide the eyes. The gray bars indicate the regions of ferromagnetic states on the EBP.

with narrow bands close to the Fermi energy may gain energy by crystal structure distortion from high-symmetry to low-symmetry structures. We suggest that a converse argument is valid in the present case. By coherency with the substrate, a high symmetry is imposed. This brings a high $D_{5f}(E_F)$ for certain values of the substrate lattice parameter a . A likely energy-lowering mechanism in such a case is the onset of ferromagnetism, since the structure is constrained.

It is worthwhile to have a closer look at the structural properties (volume and c/a ratio) of the tetragonal states constituting the EBP. In Fig. 5 we plotted $c(a)/a$ vs a , which is expected to follow a hyperbolic decrease as a is increased, if the volume is conserved under the biaxial stress. At variance with this expectation, the curve shows two rootlike anomalies. Both anomalies coincide with sharp peaks of $D(E_F)$ vs a , i.e., their electronic origin is a Van Hove singularity at the Fermi level. This means that the almost sudden change of c/a and the related volume change can be attributed to the same mechanism³⁴ that is responsible for the open structure of α -U: a competition between band energies and electrostatic terms.

The resulting strong dependence of the atomic volume on a , varying by more than 15% in the considered a range, favors magnetism. Ferromagnetic solutions occur in a range where the atomic volume is larger than in α -uranium. It is instructive in this context to compare the DOS of α -U with that of bct U; Fig. 2. Without loss of generality we chose the tetragonal state at $a = 3.00$ Å (with $c/a = 1.67$). The width of the $5f$ -dominated band is clearly narrower in the bct structure than in the orthorhombic structure due to the larger atomic volume. Moreover, the Van Hove singularities are more pronounced in the bct structure due to the imposed higher symmetry. Both effects act together, causing a high $D(E_F)$ of bct U with related magnetic instability.

It is further interesting to consider the tetragonal state lowest in total energy, bct⁽³⁾, with a calculated ratio of $c/a = 0.82$. This ratio is close to the value $\sqrt{2/3} \approx 0.816$, the ideal ratio of the so-called bct₁₀ structure. In this structure each atom has ten nearest neighbors at exactly the same distance.³⁵ For protactinium, the actinide element preceding uranium, the observed ground-state structure is bct with $c/a = 0.825$. A

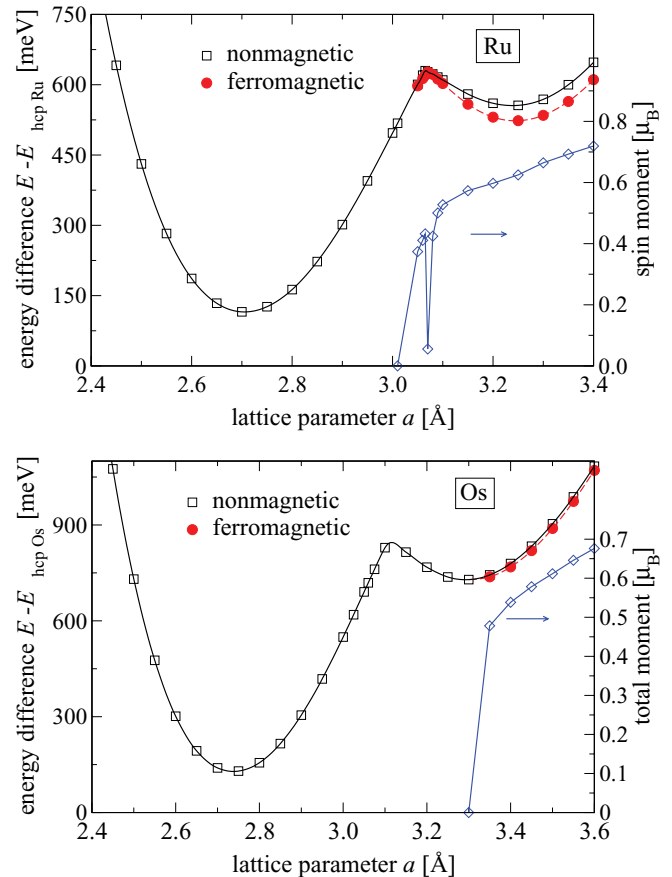


FIG. 6. (Color online) Total energy along the epitaxial Bain path of ruthenium (upper panel) and osmium (lower panel) with nonmagnetic and ferromagnetic solutions. The energy curves are spline interpolations to the data and are given with respect to the energy of the stable hcp phase $E_0 \equiv E_{\text{hcp}}$. The lines serve as guides to the eye.

predicted transformation path of α -uranium under pressure is α -U \rightarrow bct U \rightarrow bcc U. The related calculation was done with $c/a = 0.82$ for bct.²⁹ However α -uranium was found to be stable in experiment up to pressures of 100 GPa.³⁶

Encouraged by the results on uranium, we investigated the EBP of all transition metal elements including the group-3 elements Sc, Y, La, and Lu but excluding the known ferromagnets Fe, Co, and Ni, for the occurrence of unknown ferromagnetic states.³⁷ Among these 28 elemental metals, only two, Ru and Os, could be identified as showing ferromagnetic solutions on a part of the EBP in the DFT calculations, Fig. 6. In the case of Ru, we find a stable ferromagnetic state for $a \geq 3.05$ Å with an energy down to 38 meV below the nonmagnetic state. For Os, the ferromagnetic solution is stable for $a \geq 3.35$ Å and the related energy gain reaches up to 13 meV. In both cases, the magnetism is driven by a Stoner instability as in bct U. The spin moments and total moments range between $0.4 \mu_B$ and $0.7 \mu_B$ for Ru and between $0.5 \mu_B$ and $0.7 \mu_B$ for Os; see Fig. 6. In the case of Ru, there is a dip in the a dependence of the spin moment close to $a = 3.07$ Å caused by a jump in $c(a)$.³⁷ The strain energies of the bct Ru and bct Os ferromagnetic states are a factor of 2–5 larger than that of ferromagnetic bct U. However, assuming

an inverse relation between the critical film thickness and the strain energy, one can expect 10 nm films to be producible.

For all three elements, we found that ferromagnetic order is preferred against layerwise antiferromagnetic (AF1) order. In the case of uranium, the related energy difference amounts to 5 meV (checked for $a = 3.00, 3.10, 3.15,$ and 4.10 Å). For ruthenium and osmium we considered the whole a range where ferromagnetic solutions were found and obtained energy differences between AF1 and ferromagnetic order of 5–35 meV and 6–12 meV, respectively. In addition, a state with layerwise order of the type $\uparrow\uparrow\downarrow\downarrow$ was tested in the case of ruthenium (whole a range) and found to be 5–17 meV above the ferromagnetic state, but in all cases below the AF1 state.

All presented results remain qualitatively the same when the local spin density approximation is used in the parametrization of Ref. 38 instead of the GGA. For the case of uranium, we find ferromagnetic solutions for $2.90 < a < 3.05$ Å with a maximum total moment $0.12 \mu_B$ and a maximum energy difference $\Delta E = E(\text{non-spin-polarized}) - E(\text{spin-polarized}) = 1.7$ meV. For Ru, ferromagnetic order is stable for $a \geq 3.10$ Å with a maximum spin moment of $0.50 \mu_B$ and a maximum $\Delta E = 9.3$ meV. Os orders ferromagnetically for $a \geq 3.35$ Å with a maximum total moment of $0.37 \mu_B$ and a maximum $\Delta E = 0.6$ meV.

IV. CONCLUSIONS

To conclude, we predict magnetic ground states of elemental uranium, ruthenium, and osmium prepared in centered tetragonal structures with appropriate in-plane lattice spacing. This can be achieved by epitaxial growth of thick, bulklike films on suitable substrates. The feasibility of this goal has been checked by the evaluation of strain energies. While we cannot completely exclude a complicated type of antiferromagnetic order or more exotic symmetry-breaking effects, a nonmagnetic state was shown to be unstable. The expected ferromagnetic ordering temperatures are in the range of several 10 K in all three cases, with the highest value predicted for ruthenium. An interesting implication would be possible competition between superconductivity and magnetic order, since all three elements are known to be superconductors with critical temperatures close to 1 K in their ground-state phases. Finally, we note that we did not find any hint of ferromagnetic order at experimentally accessible parts of the EBP among 26 further elemental transition metals.

ACKNOWLEDGMENTS

We gratefully acknowledge discussion with Sebastian Fähler, Carsten Neise, and Ladia Havela.

*s.schoenecker@ifw-dresden.de

¹C. Buzea and K. Robbie, *Supercond. Sci. Technol.* **18**, R1 (2005).

²P. Santini, R. Lémanski, and P. Erdős, *Adv. Phys.* **48**, 537 (1999).

³L. M. Sandratskii and J. Kübler, *Phys. Rev. Lett.* **75**, 946 (1995).

⁴N. T. Huy, A. Gasparini, D. E. de Nijs, Y. Huang, J. C. P. Klaasse, T. Gortenmulder, A. de Visser, A. Hamann, T. Görlach, and H. v. Löhneysen, *Phys. Rev. Lett.* **99**, 067006 (2007).

⁵C. S. Barrett, M. H. Mueller, and R. L. Hitterman, *Phys. Rev.* **129**, 625 (1963).

⁶G. H. Lander, E. S. Fisher, and S. D. Bader, *Adv. Phys.* **43**, 1 (1994).

⁷J. Donohue, *The Structures of the Elements* (John Wiley & Sons, New York, 1974).

⁸P. Söderlind, *Phys. Rev. B* **66**, 085113 (2002).

⁹K. T. Moore and G. van der Laan, *Rev. Mod. Phys.* **81**, 235 (2009).

¹⁰L. Fast, O. Eriksson, B. Johansson, J. M. Wills, G. Straub, H. Roeder, and L. Nordström, *Phys. Rev. Lett.* **81**, 2978 (1998).

¹¹A. N. Chantis, R. C. Albers, M. D. Jones, M. van Schilfhaarde, and T. Kotani, *Phys. Rev. B* **78**, 081101(R) (2008).

¹²N. Stojić, J. W. Davenport, M. Komelj, and J. Glimm, *Phys. Rev. B* **68**, 094407 (2003).

¹³A. Laref, E. Şaşıoğlu, and L. M. Sandratskii, *J. Phys.: Condens. Matter* **18**, 4177 (2006).

¹⁴The term “bulklike” means that the film properties, except its structure, are not essentially influenced by surface or interface. For the considered case of ordered magnetism, films thicker than about ten atomic layers are bulklike.

¹⁵S. L. Molodtsov, J. Boysen, M. Richter, P. Segovia, C. Laubschat, S. A. Gorovikov, A. M. Ionov, G. V. Prudnikova, and V. K. Adamchuk, *Phys. Rev. B* **57**, 13241 (1998).

¹⁶L. Berbil-Bautista, T. Hänke, M. Getzlaff, R. Wiesendanger, I. Opahle, K. Koepernik, and M. Richter, *Phys. Rev. B* **70**, 113401 (2004).

¹⁷R. Springell, B. Detlefs, G. H. Lander, R. C. C. Ward, R. A. Cowley, N. Ling, W. Goetze, R. Ahuja, W. Luo, and B. Johansson, *Phys. Rev. B* **78**, 193403 (2008).

¹⁸S. Blügel, *Phys. Rev. Lett.* **68**, 851 (1992).

¹⁹S. Watanabe, T. Komine, T. Kai., and K. Shiiki, *J. Magn. Magn. Mater.* **220**, 277 (2000).

²⁰K. Shiiki and O. Hio, *Jpn. J. Appl. Phys.* **36**, 7360 (1997).

²¹P. Alippi, P. M. Marcus, and M. Scheffler, *Phys. Rev. Lett.* **78**, 3892 (1997).

²²P. M. Marcus, F. Jona, and S. L. Qiu, *Phys. Rev. B* **66**, 064111 (2002).

²³*Epitaxial Growth*, edited by J. W. Matthews (Academic Press, New York, 1975).

²⁴M. Wuttig and X. Liu, *Ultrathin Metal Films* (Springer, Berlin, 2004).

²⁵J. Buschbeck, I. Opahle, M. Richter, U. K. Röbber, P. Klaer, M. Kallmayer, H. J. Elmers, G. Jakob, L. Schultz, and S. Fähler, *Phys. Rev. Lett.* **103**, 216101 (2009).

²⁶M. Zelený, D. Legut, and M. Šob, *Phys. Rev. B* **78**, 224105 (2008).

²⁷K. Koepernik and H. Eschrig, *Phys. Rev. B* **59**, 1743 (1999).

²⁸J. P. Perdew, K. Burke, and M. Ernzerhof, *Phys. Rev. Lett.* **77**, 3865 (1996); **78**, 1396(E) (1997).

²⁹P. Söderlind, *Adv. Phys.* **47**, 959 (1998).

³⁰M. S. S. Brooks and P. J. Kelly, *Phys. Rev. Lett.* **51**, 1708 (1983).

³¹M. Richter, *Density Functional Theory Applied to 4f and 5f Elements and Metallic Compounds* (Elsevier, Amsterdam, 2001), Chap. 2, pp. 87–228

³²V. L. Moruzzi, *Phys. Rev. Lett.* **57**, 2211 (1986).

³³J. M. Wills and O. Eriksson, *Phys. Rev. B* **45**, 13879 (1992).

- ³⁴P. Söderlind, O. Eriksson, B. Johansson, J. M. Wills, and A. M. Boring, *Nature (London)* **374**, 524 (1995).
- ³⁵W. H. Zachariasen, *Acta Crystallogr.* **5**, 19 (1952).
- ³⁶T. Le Bihan, S. Heathman, M. Idiri, G. H. Lander, J. M. Wills, A. C. Lawson, and A. Lindbaum, *Phys. Rev. B* **67**, 134102 (2003).
- ³⁷S. Schönecker, Ph.D. thesis, TU Dresden, Germany, 2011.
- ³⁸J. P. Perdew and Y. Wang, *Phys. Rev. B* **45**, 13244 (1992).